The Journal of Experimental Biology 205, 2615–2626 (2002)
Printed in Great Britain © The Company of Biologists Limited
JEB4007



# Scaling bat wingbeat frequency and amplitude

R. D. Bullen[1,*] and N. L. McKenzie[2]

[1]*43 Murray Drive, Hillarys, Western Australia, Australia 6025* and [2]*Department of Conservation and Land Management, PO Box 51, Wanneroo, Western Australia, Australia, 6065*

*Author for correspondence (e-mail: bullen2@bigpond.com)

*Accepted 6 June 2002*

## Summary

**Wingbeat frequency ($f_w$) and amplitude ($\theta_w$) were measured for 23 species of Australian bat, representing two sub-orders and six families. Maximum values were between 4 and 13 Hz for $f_w$, and between 90 and 150 ° for $\theta_w$, depending on the species. Wingbeat frequency for each species was found to vary only slightly with flight speed over the lower half of the speed range. At high speeds, frequency is almost independent of velocity. Wingbeat frequency (Hz) depends on bat mass ($m$, kg) and flight speed ($V$, m s$^{-1}$) according to the equation: $f_w=5.54–3.068\log_{10}m–2.857\log_{10}V$. This simple relationship applies to both sub-orders and to all six families of bats studied. For 21 of the 23 species, the empirical values were within 1 Hz of the model values. One species, a small molossid, also had a second mode of flight in which $f_w$ was up to 3 Hz lower for all flight speeds.**

**The following relationship predicts wingbeat amplitude to within ±15 ° from flight speed and wing area ($S_{REF}$, m$^2$) at all flight speeds: $\theta_w=56.92+5.18V+16.06\log_{10}S_{REF}$. This equation is based on data up to and including speeds that require maximum wingbeat amplitude to be sustained. For most species, the maximum wingbeat amplitude was 140 °.**

Key words: bat, scaling, wingbeat, frequency, amplitude.

## Introduction

Chiroptera cover both tropical and temperate regions and reach high latitudes. One of the main constraints on their geographical radiation is their energy balance. The daily cycle of energy expenditure in bats is dominated by the cost of foraging flight, which is a function of their aerodynamics and, hence, their wingbeat frequency and amplitude across the range of normal flight speeds. These data are only available for a few species (Norberg et al., 1993; Aldridge, 1986; Van Den Berg and Rayner, 1995; Britton et al., 1997; Carpenter, 1986; Norberg, 1976). To improve our understanding of bat energetics, a general model is required that is scaled to a readily available parameter such as species mass and that encompasses bats from an array of climatic zones and with a range of foraging strategies.

In mammals, the duration of a muscle's contraction is adapted to its function, and the contraction performance of the muscle is affected by the resistance that it works against (Guyton and Hall, 1996). If there were gross variations in the speed of operation of the muscles driving the wingbeat of bats with different phylogenetic relationships, foraging strategies or microhabitats, then we would expect the relationships between wingbeat frequency ($f_w$) and airframe variables (such as mass, wing area and wing span) to be complex.

In this study, we measure wingbeat frequency and amplitude across a range of flight speeds for 23 species representing all families of insectivorous, frugivorous and carnivorous bats that occur in tropical and temperate regions of Western Australia. We then propose a general model linking these variables to various airframe attributes and flight speed.

## Materials and methods

### *Study animals*

The 23 species of Australian bat assessed in this study are listed below, together with authorities and synonyms in cited references. Table 1 gives morphological parameters and Table 2, foraging niche, climatic range and phylogeny, for each species.

*Chalinolobus gouldii* Grey; *Chalinolobus morio* Grey; *Chalinolobus nigrogriseus* Gould; *Hipposideros ater*, Templeton; *Macroderma gigas* Dobson; *Mormopterus planiceps* Peters; *Miniopterus schreibersii* Kuhl; *Nyctophilus arnhemensis* Johnson; *Nyctophilus geoffroyi* Leach; *Nyctophilus gouldi* Tomes; *Nyctophilus timoriensis* Geoffroy; *Pteropus poliocephalus* Temminck; *Pteropus scapulatus* Peters; *Rhinonycteris aurantius* Grey; *Scotorepens balstoni* Thomas; *Saccolaimus flaviventris* Peters; *Scotorepens greyii* Grey (previously *Nycticeius balstoni caprenus* Troughton); *Tadarida australis* Grey; *Taphozous georgianus* Thomas; *Taphozous hilli* Kitchener; *Vespadelus finlaysoni* Kitchener, Jones and Caputi (previously *Eptesicus pumilis* Gray); *Vespadelus regulus* Thomas.

Table 1. *Primary flight performance parameters (mean values) for species included in the study*

| Species | *N* | Mass, *m* (kg) | Wing span (m) | Wing area, $S_{REF}$ ($m^2$) | Aspect ratio, $span^2/S_{REF}$ | Wing loading, weight/$S_{REF}$ ($N\,m^{-2}$) |
|---|---|---|---|---|---|---|
| *Chalinolobus gouldii*[a] | 24 | 0.0134 | 0.3457 | 0.01788 | 6.70 | 7.35 |
| *Chalinolobus morio*[a] | 13 | 0.0070 | 0.2877 | 0.01351 | 6.14 | 5.08 |
| *Chalinolobus nigrogriseus*[c] | 1 | 0.0065 | 0.2780 | 0.01218 | 6.35 | 5.24 |
| *Hipposideros ater*[e] | 13 | 0.0044 | 0.2489 | 0.01061 | 5.84 | 4.07 |
| *Macroderma gigas*[e] | 5 | 0.130 | 0.7590 | 0.09478 | 6.08 | 13.44 |
| *Miniopterus schreibersii*[e] | 15 | 0.0101 | 0.3409 | 0.01674 | 6.94 | 5.91 |
| *Mormopterus planiceps*[a] | 8 | 0.0086 | 0.2635 | 0.00959 | 7.25 | 8.69 |
| *Nyctophilus arnhemensis*[c] | 1 | 0.0071 | 0.3014 | 0.01561 | 5.82 | 4.46 |
| *Nyctophilus geoffroyi*[a] | 12 | 0.0057 | 0.2631 | 0.01222 | 5.68 | 4.74 |
| *Nyctophilus gouldi*[d] | 17 | 0.0100 | 0.3046 | 0.01597 | 5.82 | 6.14 |
| *Nyctophilus timoriensis*$_g$[a] | 12 | 0.0110 | 0.3219 | 0.01734 | 5.98 | 6.22 |
| *Nyctophilus timoriensis*$_{s/w}$[e] | 8 | 0.0142 | 0.3495 | 0.02027 | 6.03 | 6.88 |
| *Pteropus poliocephalus*[e] | 1 | 0.700 | 1.338 | 0.2582 | 6.93 | 26.59 |
| *Pteropus scapulatus*[e] | 3 | 0.412 | 1.106 | 0.1650 | 7.41 | 24.50 |
| *Rhinonycteris aurantius*[e] | 5 | 0.0086 | 0.3080 | 0.01507 | 6.29 | 5.60 |
| *Saccolaimus flaviventris*[b] | 4 | 0.0462 | 0.5750 | 0.03945 | 8.38 | 11.49 |
| *Scotorepens balstoni*[a] | 9 | 0.0080 | 0.2660 | 0.01130 | 6.27 | 6.95 |
| *Scotorepens greyi*[b] | 5 | 0.0070 | 0.2500 | 0.01010 | 6.19 | 6.80 |
| *Tadarida australis*[a] | 9 | 0.0353 | 0.4625 | 0.02584 | 8.28 | 13.40 |
| *Taphozous georgianus*[c] | 11 | 0.0281 | 0.4637 | 0.02811 | 7.74 | 9.81 |
| *Taphozous hilli*[e] | 11 | 0.0241 | 0.4616 | 0.02736 | 7.79 | 8.64 |
| *Vespadelus finlaysoni*[b] | 2 | 0.0056 | 0.2549 | 0.01042 | 6.24 | 5.27 |
| *Vespadelus regulus*[a] | 13 | 0.0047 | 0.2335 | 0.00891 | 6.12 | 5.17 |

[a]Bullen and McKenzie (2001); [b]R. D. Bullen and N. L. McKenzie, unpublished data; [c]McKenzie et al. (1995a); [d]Fullard et al. (1991); [e]this study.

Although measurements are based on a single animal, *Pteropus poliocephalus* is included as an equivalent to the 700 g fruit bat studied by Carpenter (1985).

Refer to Materials and methods for the explanation of the two different populations of *Nyctophilus timoriensis*.

Data for two different populations of *Nyctophilus timoriensis* ($Nt_g$ and $Nt_{s/w}$) are presented and treated as separate species. The arid population $Nt_g$ inhabits the Coolgardie woodlands and has a mean mass of 11 g, whereas the mesic population $Nt_{s/w}$ is endemic to the forests of southwestern Western Australia and has a mean mass of 14.2 g.

### *Data collection*

Relevant aspects of species foraging ecologies and airframe measures were collected from existing literature. Only publications using a consistent measurement technique were used. This measurement protocol, relevant formulae and a discussion of aerodynamic mechanisms and implications are provided in Bullen and McKenzie (2001). Capture and release techniques were used to collect a library of video recordings complete with flight speed measurements. Bat flight was filmed using video cameras (Sony Video8 Professional CCD-V100E in VHS format and Sony digital Beta-cam model DVW-709WSP at a shutter speed of 1/250 s), both running at 24 frames $s^{-1}$. Wingbeat frequency and amplitude values were determined from a frame-by-frame playback. Note that the Beta format video actually showed two clear images of the bats wing position when replayed *via* VHS because of the differences in the recording protocols of the two video standards. It gives an effective frame rate of 48 frames $s^{-1}$ for test points recorded with the DigiBeta camera. Limited data were also collected in an indoor observation chamber at high frame rates using a cine camera running at 200 frames $s^{-1}$ (Photosonics; Burbank, CA, USA; model 61-1100).

Flight speeds were measured continuously in all cases using a hand-held K-band radar gun (model TS3, Municipal Electronics, UK, calibrated for a speed range of 1–28 m $s^{-1}$). These speeds were ‘called’ into a hand-held recorder and, if applicable, into the audio feature of the video camera while each test animal was being filmed. For each test, the angle between the gun’s line of sight to the bat and the bat’s line of flight was estimated by the operator and ‘called’ into the recorder. A cosine correction was applied to the measured flight speeds to correct for this angle. Data corresponding to angles greater than 45 ° were ignored.

The mean angle of the wing between shoulder and tip, above or below the body axis reference dorsal plane, was estimated within ±5 ° for each frame in sequence. Note that this method is different from that used by Pennycuick (1996) on birds. Pennycuick (1996) estimated the angle created by the shoulder-to-wrist joint line only. A bat’s hand wings reaches higher

Table 2. *Foraging niche, climatic range and phylogeny for species included in the study*

| Species | Usual foraging strategy[1] | Usual foraging Micro-habitat[1] | Range | Family |
|---|---|---|---|---|
| *Chalinolobus gouldii* | A[1, 5] | BS/O[1,2] | Tr, Te, a, m | V |
| *Chalinolobus morio* | A[1] | BS/A [1] | Te, a, m | V |
| *Chalinolobus nigrogriseus* | A[6] | BS/O [2] | Tr, m | V |
| *Hipposideros ater* | S[1] | BS/A[2,5] | Tr, m | H |
| *Macroderma gigas* | I, S[1] | BS/O[4,5] | Tr, a, m | Ma |
| *Miniopterus schreibersii* | A[1] | BS/O[2], AC[5] | Tr, m | V |
| *Mormopterus planiceps* | I[1] | AC[1] | Te, a, m | Mo |
| *Nyctophilus arnhemensis* | S[1] | IS[2] | Tr, m | N |
| *Nyctophilus geoffroyi* | S[1,5] | BS/A-IS[1,2] | Tr, Te, a, m | N |
| *Nyctophilus gouldi* | S[7] | BS/A-IS[7] | Te, m | N |
| *Nyctophilus timoriensis*$_g$ | S[1] | BS/A-IS[1] | Te, a | N |
| *Nyctophilus timoriensis*$_{s/w}$ | S[7] | BS/A-IS[7] | Te, m | N |
| *Pteropus poliocephalus* | F[5] | AC[5] | Tr, Te, m | P |
| *Pteropus scapulatus* | F[5] | AC[5] | Tr, m, a | P |
| *Rhinonycteris aurantius* | A[1] | BS/A[1] | Tr, a, m | H |
| *Saccolaimus flaviventris* | A[1,5] | AC[1,3] | Tr, a, m | E |
| *Scotorepens balstoni* | A[1] | BS/O[1] | Te, a | V |
| *Scotorepens greyi* | A[1,6] | BS/O[2,3,5] | Tr, a, m | V |
| *Tadarida australis* | I[1,5] | OC[1,2,3] | Tr, a; Te, m | M |
| *Taphozous georgianus* | A[5] | OC[2,3] | Tr, a, m | E |
| *Taphozous hilli* | A[7] | OC[7] | Tr, Te, a | E |
| *Vespadelus finlaysoni* | A[1,5] | BS/A[1,2,3,7] | Tr, Te, a | V |
| *Vespadelus regulus* | A[1] | BS/A[1] | Te, a, m | V |

[1]Bullen and McKenzie (2001); [2]McKenzie and Start (1989); [3]McKenzie and Muir (2000); [4]McKenzie et al. (1995a); [5]Churchill (1998); [6]Fenton (1982); [7]this study.

A, air superiority; I, interceptor; S, surface; F, frugivore; OC, over canopy; AC, above canopy; BS/O, beside stand in open; BS/A beside stand, against clutter; IS, inside stand; Tr, tropical; Te, temperate; a, arid; m, mesic; E, Emballonuridae; H, Hipposideridae; Ma, Megadermatidae; Mo, Molossidae; P, Pteropodidae; V, Vespertilionidae (includes N, Nyctophilinae).

*Macroderma gigas* is known to forage using both interceptor and surface strategies equally.

Refer to Materials and methods for the explanation of the two different populations of *Nyctophilus timoriensis*.

positional angles than its arm wing at the end of the stroke, so our method gives higher amplitude values. These were plotted against time (Fig. 1) and fitted with splines using Microsoft EXCEL. A minimum of three complete wingbeat cycles was required to calculate frequency, $f_w$, and amplitude, $\theta_w$, reliably. At 24 frames $s^{-1}$, a family of lines can be fitted to the sequences, differing in their frequencies by a factor of 3. Given that bats with a mass of less than 50 g are known to use $f_w$ in the range of 3–12 Hz (Carpenter, 1985; Van Den Berg and Rayner, 1995), the curve with the lowest $f_w$ was used for all species because its frequency always fell within this range. This also agrees with our own high frame rate data. The $f_w$ information was then deduced directly from the time histories. The spline for each low frame rate (VHS at 24 frames $s^{-1}$) test point was reviewed to obtain amplitude. The maximum and minimum amplitudes were then averaged and compared to give $\theta_w$ values for each test point. Given that the test points were all taken during periods approximating steady level flight, peaks that were clearly out of phase with the sequence were ignored in this average (see Fig. 1B). This method is expected to give maximum and minimum $\theta_w$ values slightly lower in magnitude than those obtained from high frame rate (>100 frames $s^{-1}$) cine cameras. Because of the impracticability of extensive use of high-frame-rate cine in the majority of our field experimental situations, this was not attempted, and low-frame-rate video was used to maximise data collection. See discussion below of the effect of this procedure on the results.

Sub-adults, pregnant females and animals with damaged wings, or that were visibly distressed or considered significantly underweight, were excluded. The methods used did not result in injury to or the death of the bats tested.

Four strategies were used to collect wingbeat data over a wide range of flight speeds. First, bats were flown in a flight chamber to collect low-speed data. Individual adult bats were released to fly around in a large, well-lit room (11 m long, 5 m wide and 3.2 m high). All species were able to maintain continuous level flight in this room. Although *Mormopterus planiceps*, *Chalinolobus gouldii* and *Tadarida australis* did not achieve their typical in-field flight speeds (see Bullen and McKenzie, 2001), they were flying 0.3–3 m $s^{-1}$ (1–10 km $h^{-1}$) above their usual minimum steady level flight speed (R. D. Bullen and N. L. McKenzie, unpublished data). Thus, they had a considerable margin of power for manoeuvring. The floor, ceiling and walls of the room were painted in shades of white or cream, which contrasted with the brown and black colours of the fur and wing membranes of the bats. This method gave excellent coverage of the lower speed range of the bats.

Second, free-air hand releases in daylight were used to collect mid- and high-speed data. The same video and speed measuring equipment was used. The bats were prone to escape after release by accelerating to high speed. Results were most readily obtained when the released bat was filmed against bright, monotonous backgrounds such as grass or sky. The initial period of 2–3 s, while bats accelerated from rest to their normal flight speed range, was excluded from data analysis. If, during the test point, the speed of the bat varied marginally (typically less than ±1 m $s^{-1}$), then the speed at the mid-point of the run was taken as the average value for that run. If the speed varied by more that ±1 m $s^{-1}$ then the run was broken into two or more test points. All readings for a species were pooled.

Third, daytime free-flying data were collected from large pteropodids as they commuted from roost to roost. Because of their size, it was possible to film the bats in flight in full daylight and to record their speed. Again, cosine corrections were applied to the measured flight speeds, as described above, to account for the off line-of-sight measurement errors.

Fourth, night-time free-flight data were also collected to supplement the first two strategies and to check whether different wingbeat values were obtained in a natural situation. Echolocation recordings were taken from free-flying bats in

situations while the foraging bat could be seen, lines of flight estimated and speeds measured. An Anabat II ultrasound detector (Titley Electronics, Australia) was used with its output stored directly onto audiocassette tapes using a Sony Walkman Professional (WMD6C) tape recorder. The species identity and $f_w$ values were then derived from the recorded call sequences using COOL EDIT 2000 (Syntrillium Software, USA). The species was identified by reference to a library of reference calls, and the $f_w$ data were derived based on a direct correlation of the wingbeat frequency with the echolocation call rate (Lancaster et al., 1995). These sequences were not filmed and did not provide data on $\theta_w$.

Of the 23 species represented in this study, 11 provided data over the flight speed range of 3–9 m s$^{-1}$ that is the majority of their speed range. Seven species provided data over the range less than 6 m s$^{-1}$, covering their low-speed range only, and five provided data at speeds greater than 5 m s$^{-1}$, which is their high-speed range only. Despite having scant or incomplete data sets, these last two categories were included to assess whether the generalised scaling model applied to all types of bat.

The $f_w$ and $\theta_w$ data for each species were then plotted against flight speed (refer, for an example plot, to Fig. 2) and the plots reviewed for a general pattern.

Maximum range speed, $V_{mr}$, was calculated and used as a reference point for low-speed flight using a quasi-steady aerodynamic model that follows the method of Pennycuick (1989). The calculated values are included in Table 3. $V_{mode}$, the 'mode' speed of the test data (Bullen and McKenzie, 2001) was estimated empirically from the data to represent the divide between low and high-speed flight. Means and standard deviations for $f_w$ corresponding to $V_{mr}$ ±1.0 m s$^{-1}$ were calculated and plotted against mass. A series of forward stepwise least-squares regression curves was tested against the frequency and flight speed data (STATISTICA SoftStat). A range of relevant morphological variables, including mass, span and wing area, was assessed as independent variables. Linear, polynomial and logarithmic variants were assessed for explaining the variation. Statistically significant relationships between $\theta_w$ and the available morphological variables were also sought.

Previously published wingbeat data for a number of other species are included for comparison: *Eidolon helvum* (*m*=315 g), high-speed cine data (Carpenter, 1986); *Hypsignathus monstrosus* (*m*=260 g), high-speed cine data (Carpenter, 1986); *Myotis dasycneme* (*m*=20 g), stroboscopic flash data at 30 Hz (Britton et al., 1997); *Noctilio leporinus* (*m*=70 g), synchronised cameras at 20 frames s$^{-1}$ (Schnitzler et al., 1994); *Pipistrellus pipistrellus* (*m*=5 g), high-speed video at 250 frames s$^{-1}$ (Thomas et al., 1990); *Pteropus poliocephalus* (*m*=700 g), manual and high-speed cine data (Carpenter, 1985); *Rhinolophus ferrumequinum* (*m*=22 g), stroboscopic flash data at 100 and 200 Hz (Aldridge, 1986); *Rousettus aegyptiacus* (*m*=180 g), high-speed cine data (Carpenter, 1986).

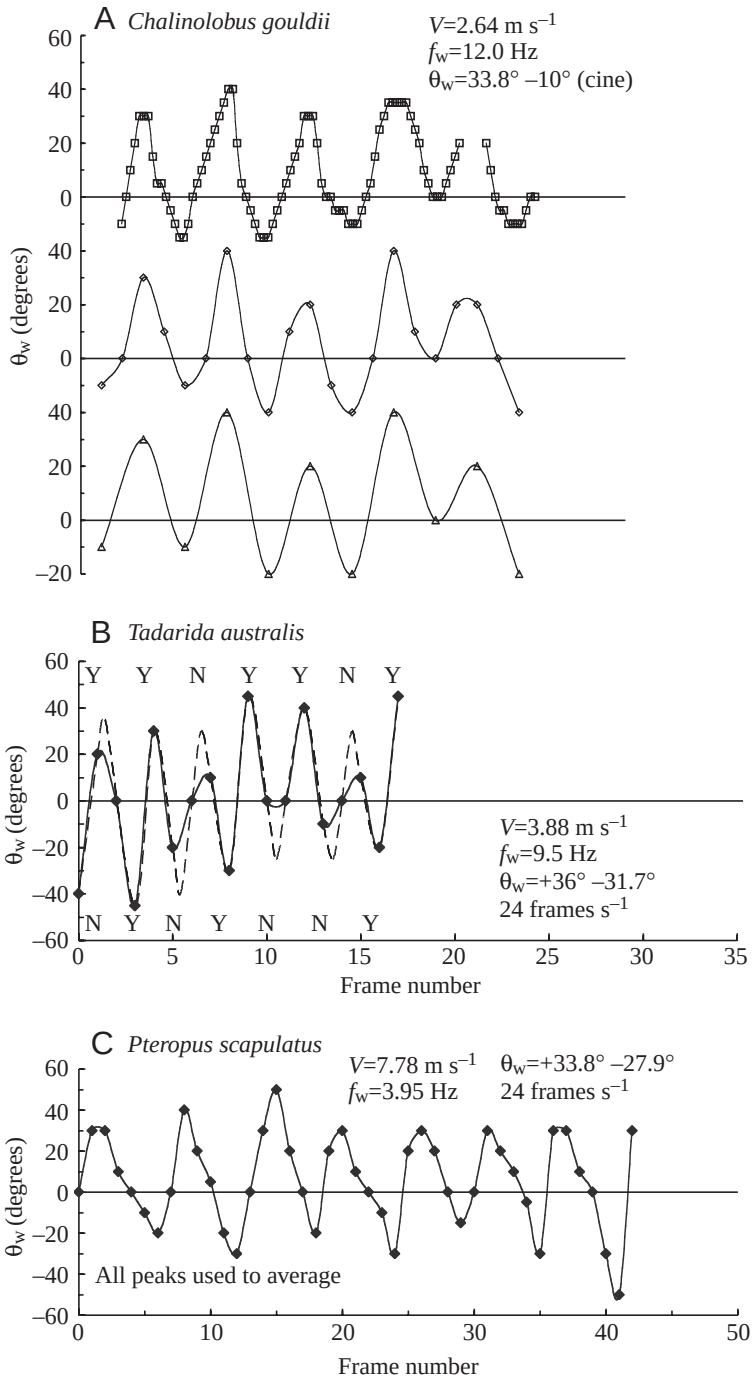


Fig. 1. Examples of wingbeat test point time histories. (A) A comparison of three recording formats at different frame rates recorded at the same time. The DigiBeta at 48 frames s$^{-1}$ (diamonds) and VHS at 24 frames s$^{-1}$ (triangles) sequences are offset from the cine recording at 200 frames s$^{-1}$ (squares) for clarity. (B,C) Typical time histories of a large microbat (B) and a megabat (C) at low frame rates. The solid line in each case is a typical spline fit applied to the data. The broken lines in B are the author's interpolation. In B, Y and N denote the peaks used and not used, respectively, in the average amplitude range assessment. *V*, flight speed; $f_w$, wingbeat frequency; $\theta_w$, wingbeat amplitude.

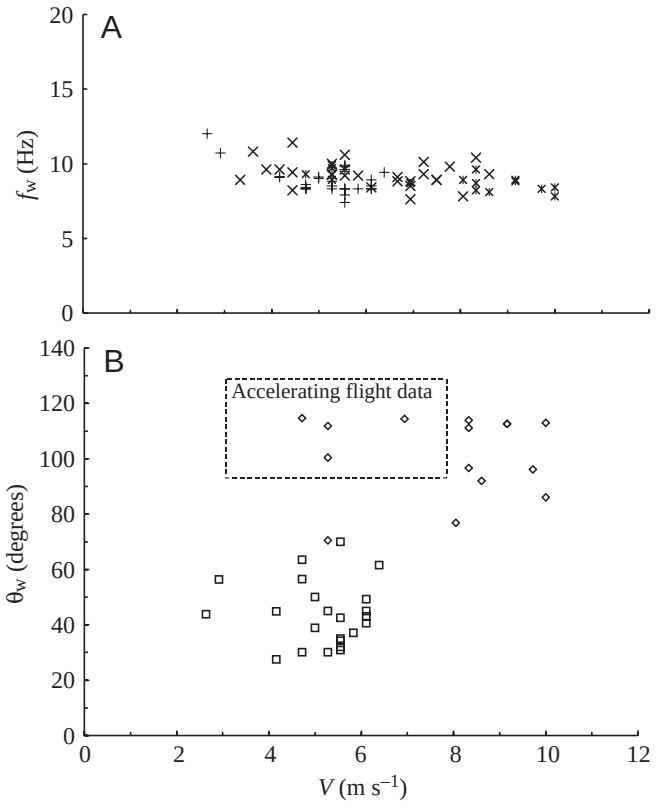


Fig. 2. Example of (A) wingbeat frequency ($f_w$) and (B) amplitude ($\theta_w$) data for one of the species included in the study, *Chalinolobus gouldii* (mass 0.0134 kg). Note this figure includes high-amplitude data (boxed points in B) taken from test points during accelerating flight at low-flight speed, because we have included them in the derivation of the maximum amplitude results in Table 5. They are not included in the derivation of the general amplitude *versus* flight speed ($V$) relationship of Equation 4. In A, + symbols are $f_w$ data from the observation chamber; x symbols, free flight $f_w$ data; crossed x symbols, hand-release test points. In B, squares are data from the observation chamber and diamonds are daylight hand-release data.

Table 3. *Flight speed values available for each species*

| Species | $N$ | $n$ | Calculated $V_{mr}$ (m s$^{-1}$) | Measured $V_{mode}$ (m s$^{-1}$) |
|---|---|---|---|---|
| *Chalinolobus gouldii* | >30 | 1118 | 4.2 | 6.7 |
| *Chalinolobus morio* | >30 | 788 | 3.6 | 5.3 |
| *Chalinolobus nigrogriseus* | 7 | 41 | 3.6 | 5.3 |
| *Hipposideros ater* | >30 | 618 | 2.2 | Insufficient free air data* |
| *Macroderma gigas* | >30 | 272 | 4.2 | 6.9 |
| *Miniopterus schreibersii* | >30 | 49 | 4.2 | 5.8 |
| *Mormopterus planiceps* | 17 | 512 | 4.2 | 8.1 |
| *Nyctophilus arnhemensis* | 4 | 337 | 2.5 | Insufficient data |
| *Nyctophilus geoffroyi* | >30 | 375 | 2.5 | 4.7 |
| *Nyctophilus gouldi* | 7 | 256 | 3.1 | 5.3 |
| *Nyctophilus timoriensis*$_g$ | 10 | 248 | 2.8 | 5.6 |
| *Nyctophilus timoriensis*$_{s/w}$ | 2 | 118 | 2.5 | Insufficient data |
| *Pteropus poliocephalus* | 7 | 17 | 5.6 | 7.5 |
| *Pteropus scapulatus* | >30 | 236 | 5.6 | 7.8 |
| *Rhinonycteris aurantius* | >30 | 699 | 4.2 | 5.8 |
| *Saccolaimus flaviventris* | >30 | 148 | 3.6 | 7.5 |
| *Scotorepens balstoni* | 10 | 399 | 3.6 | 6.1 |
| *Scotorepens greyi* | 27 | 137 | 4.2 | 5.8 |
| *Tadarida australis* | >30 | 372 | 5.3 | 8.3 |
| *Taphozous georgianus* | 19 | 183 | 3.9 | 6.1 |
| *Taphozous hilli* | >30 | 301 | 3.6 | 5.3 |
| *Vespadelus finlaysoni* | >30 | 1018 | 3.1 | 5.3 |
| *Vespadelus regulus* | >30 | 677 | 3.6 | 5.0 |

Measured data are pooled across Western Australian regions.

Mode flight speed data were collected as described by Bullen and McKenzie (2001).

The $V_{mr}$ values were estimated using a quasi-steady aerodynamic model consistent with Pennycuick (1989).

$N$, number of specimens; $n$, number of observations.

*Majority of speeds were recorded inside the mouth of a roosting cave, biasing the $V_{mode}$ estimate.

Refer to Materials and methods for the explanation of the two different populations of *Nyctophilus timoriensis*.

## Results

Data on foraging ecology and airframe variables were available for Western Australian populations of 22 species and for a southeastern Australian population of *Pteropus poliocephalus*. Morphological variables are listed in Table 1. The foraging strategy, biogeographical and phylogenetic data for the species are given in Table 2 (terms are defined in Bullen and McKenzie, 2001). Table 3 provides calculated $V_{mr}$ and measured $V_{mode}$ flight speeds for each species.

An example of the $f_w$ and $\theta_w$ data for *Chalinolobus gouldii* is given in Fig. 2 and a second example for $f_w$, *Mormopterus planiceps*, is given in Fig. 6. For all 11 species assessed over a wide range of flight speed, $f_w$ initially decreased with increasing speed until a mid-range speed was reached. $f_w$ then remained relatively constant until high speeds were achieved. This pattern can also be seen clearly in Figs 2A and 6. Regarding amplitude, Fig. 2 also illustrates a pattern common to all 11 species: $\theta_w$ increased with speed, although there was very wide scatter.

### *Estimation of wingbeat frequency*

A summary plot of the relationship at low flight speeds between $f_w$ and mass ($m$) is presented in Fig. 3A. The $f_w$ values correspond to $V_{mr}$ that is approximately midway through the flight-speed region that exhibits the distinct reduction of $f_w$. The line of best fit for $f_w$ is also given. Fig. 3A shows good correlation between $f_w$ at low speed and mass. The relationship is convenient to use for estimating $f_w$ in bats at low speed and is given for $V$=$V_{mr}$ by:

$$f_w = 3.65 - 3.312\log_{10}m\,, \quad (1)$$

with $r^2$=0.875, $P$<0.00001, ±0.863 Hz (estimated S.E.M.).

At high flight speeds, mass was again a good predictor of $f_w$ (Fig. 3B). Excluding the two outliers (discussed below), the line of best fit for $V>6\,m\,s^{-1}$ was:

$$f_w = 2.40 - 3.444\log_{10}m\,, \qquad (2)$$

with $r^2$=0.905, $P$<0.00001, ±1.04 Hz (estimated S.E.M.).

Provided bat mass is known, the wingbeat frequency for any bat can be estimated at low or high flight speed to within ±1.5 Hz.

To improve the fidelity of the estimate and to provide a general relationship across all speeds, we applied a multiple-parameter least-squares regression analysis to the full data set and a range of morphological variables. Using $f_w$, $m$ and flight speed ($V$), a linear model explained 65.0 % of the variation ($P$<0.00001, ±1.24 Hz). Including span and area in this model improved the fit slightly to explain 73.0 % of the variation ($P$<0.00001, ±1.09 Hz). A scatterplot of $f_w$ *versus* flight speed suggested that more of the variation would be explained by using a non-linear model. We therefore evaluated polynomial and logarithmic fits. Including $\log_{10}m$ and $\log_{10}V$ increased the $r^2$ values to 0.748. Including span and area did not significantly improve the fit. Wingbeat frequency is then given over the full flight speed and mass ranges by:

$$f_w = 5.54 - 3.068\log_{10}m - 2.857\log_{10}V\,, \qquad (3)$$

$r^2$=0.748, $P$<0.00001, estimated S.E.M. ±1.05 Hz, $F$=545; S.E.M. intercept=0.31 Hz, $P$<0.00001; S.E.M. $\log_{10}m$=0.11, $P$<0.00001; S.E.M. $\log_{10}V$=0.27, $P$<0.00001.

This model is presented in Fig. 4.

Equation 3 is presented in Fig. 5 for *Chalinolobus gouldii*, for comparison with the data of Fig. 2.

The two outliers in Fig. 3B have high-speed $f_w$ values significantly below the line represented by this equation. They are *Mormopterus planiceps* (this study) and *Noctilio leporinus* (Schnitzler et al., 1994), which have $f_w$ values corresponding to approximately 65 % of the value predicted by Equation 2. Our empirical data on *Mormopterus planiceps* are presented in Fig. 6. The *Mormopterus planiceps* outlier is a series of low $f_w$ points treated separately. The upper series in Fig. 6 is accurately represented by the scaling equations.

A summary of the data included in the study is given in Table 4.

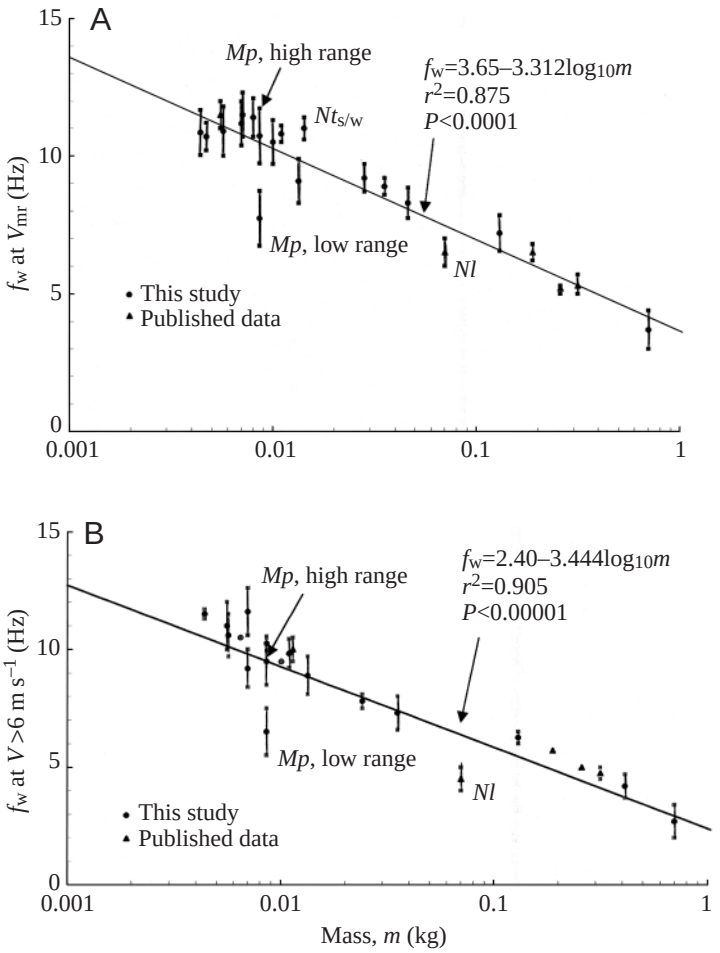


Fig. 3. Summary of wingbeat frequency ($f_w$) data. (A) Low-speed data. For each species, the mean values ± S.D. of the data at maximum range velocity ($V_{mr}$) are presented. The linear regression curve may be used to estimate $f_w$ at $V_{mr}$ for all species. (B) High-speed data. For each species, the mean value ± S.D. of the data ($V>6\,m\,s^{-1}$) are presented. The linear regression curve may be used to estimate $f_w$ for all species flying at high speeds. *Mp*, *Mormopterus planiceps*, *Nt*$_{s/w}$, the southwestern population of *Nyctophilus timoriensis* and *Nl*, *Noctilio leporinus*.

*Estimation of wingbeat amplitude*

When variation in wingbeat amplitude was evaluated against flight speed and morphological variables, flight speed ($V$) and wing area ($S_{REF}$) explained most of the variation (Fig. 7A).

$$\theta_w = 56.92 + 5.18V + 16.06\log_{10}S_{REF}\,, \qquad (4)$$

$r^2$=0.417, ±14.86 °, $P$<0.00001, $f$=104.73; S.E.M. intercept=6.81, $P$<0.00001; S.E.M. $V$=0.43, $P$<0.00001; S.E.M. $\log_{10}S_{REF}$=3.40, $P$<0.00001.

Equation 4 is presented in Fig. 5 for *Chalinolobus gouldii* for comparison with the data of Fig. 2.

The maximum and minimum values of $\theta_w$ recorded during the study are presented in Table 5 for each species. They are much higher than the extrapolations based on Equation 4. This is to be expected given that pectoral girdle anatomy clearly permits very high $\theta_w$ values to be used for extreme speeds beyond our data set as well as during manoeuvres and periods of high acceleration when extra power is required. For the reasons given in the legend to Fig. 2, low flight speed test points at amplitudes approaching the maximum and minimum values were observed (typically +40 and –80 °), but were not included in the derivation of Equation 4.

## Discussion

We have derived a general model for calculating wingbeat frequency and amplitude of bats in their usual speed range. The $f_w$ equations require only mass and flight speed to provide accurate estimates for a species. The $\theta_w$ equation is less

Table 4. *Summary of data included in this study*

| Species | Speed range ($m\,s^{-1}$) | *N* | *n* | *t* | *c* | Wingbeat frequency $f_w$ (Hz) | Wingbeat amplitude $\theta_w$ (degrees) | Coasting observed |
|---|---|---|---|---|---|---|---|---|
| *Chalinolobus gouldii* | 3.3–10.0 | 40 | 70 | 244 | 6.10 | 9.04±0.87 | 65.48±31.56 | Yes |
| *Chalinolobus morio* | 2.2–7.8 | 4 | 14 | 118 | 6.94 | 10.91±1.01 | 49.23±15.39 | Yes |
| *Chalinolobus nigrogriseus* | 5.6–9.4 | 4 | 4 | 35 | 8.75 | 11.27±0.84 | 56.67±15.28 | Yes |
| *Hipposideros ater* | 2.2–4.7 | 9 | 20 | 75 | 8.33 | 10.91±0.80 | 57.14±8.88 | No |
| *Macroderma gigas* | 2.8–8.1 | 1 | 8 | 60 | 6.67 | 6.96±0.71 | 83.75±18.47 | No |
| *Miniopterus schreibersii* | 5.8–8.9 | 1 | 2 | 25 | 12.5 | 9.10±0.57 | 92.50±17.68 | No |
| *Mormopterus planiceps* | 2.1–9.4 | 34 | 72 | 211 | 6.81 | 9.34±1.38 | 40.68±10.15 | Yes |
| *Nyctophilus arnhemensis* | 1.1–4.7 | 2 | 31 | 259 | 8.35 | 11.43±1.13 | 33.44±11.18 | Yes |
| *Nyctophilus geoffroyi* | 0.8–7.2 | 6 | 23 | 163 | 9.88 | 10.94±0.96 | 43.92±16.44 | Yes |
| *Nyctophilus gouldi* | 1.7–5.8 | 6 | 22 | 221 | 10.52 | 10.40±1.05 | 59.29±10.99 | Yes |
| *Nyctophilus timoriensis*$_g$ | 1.4–6.7 | 4 | 17 | 224 | 13.93 | 10.56±0.59 | 48.80±18.74 | Yes$^\dagger$ |
| *Nyctophilus timoriensis*$_{s/w}$ | 1.7–2.5 | 2 | 10 | 150 | 15.0 | 11.08±0.34 | 47.50±5.40 | Yes |
| *Pteropus poliocephalus* | 3.1–8.6 | 3 | 15 | 21 | 7.0 | 3.40±0.88 | 86.67±12.58 | No |
| *Pteropus scapulatus* | 6.7–10.0 | 7 | 7 | 40 | 5.71 | 4.15±0.50 | 94.29±17.18 | Yes |
| *Rhinonycteris aurantius* | 2.5–7.2 | 5 | 13 | 156 | 9.18 | 9.76±0.55 | 70.77±14.12 | Yes |
| *Saccolaimus flaviventris* | 1.7–5.3 | 1 | 12 | 91 | 5.92 | 8.36±0.75 | 48.33±8.66 | No |
| *Scotorepens balstoni* | 3.3–5.0 | 1 | 9 | 64 | 10.69 | 11.31±0.67 | 35.00±8.29 | No |
| *Scotorepens greyi* | 6.7–8.3 | 7 | 7 | 80 | 13.0 | 11.59±1.01 | 60.00±18.26 | Yes |
| *Tadarida australis* | 3.6–13.5 | 14 | 23 | 154 | 9.6 | 8.19±1.08 | 90.74±27.70 | No |
| *Taphozous georgianus* | 2.5–4.2 | 1 | 5 | 44 | 8.8 | 8.00±1.89 | 71.00±7.42 | No |
| *Taphozous hilli* | 6.1–8.3 | 6 | 6 | 58 | 8.29 | 7.47±0.46 | 100.00±8.94 | No |
| *Vespadelus finlaysoni* | 4.7–8.1 | 12 | 12 | 88 | 6.77 | 10.68±1.11 | 58.18±9.82 | No |
| *Vespadelus regulus* | 1.4–6.9 | 7 | 14 | 145 | 10.52 | 10.75±0.57 | 41.38±6.85 | No |

*N*, the number of individual animals tested for each species; *n*, the number of test points for each species; *t*, the total number of wingbeat cycles recorded with amplitude data; *c*, the mean number of wingbeat cycles per test point.

Coasting refers to the observed use of intermittent periods of wing flapping during the video recordings.

$^\dagger$*Nyctophilus timoriensis*$_g$ has also been observed using bounding flight at high speeds.

Values for $f_w$ and $\theta_w$ are means ± S.D.

Refer to Materials and methods for the explanation of the two different populations of *Nyctophilus timoriensis*.

accurate and requires flight speed and wing area. These equations apply to steady, level flight in the range of speeds given in Table 4, but exclude the high and low extremes of the bat's speed range. They apply to bats from a wide range of environments and with very different foraging strategies and phylogenetic affiliations.

Strong family-level phylogenetic relationships are apparent in our results. Vespertilionidae are at one end of the relationship, Emballonuridae in the middle and Pteropodidae at the opposite end. Given the high selective pressures on morphological characters associated with modes of nutrition and foraging, phylogeny in the absence of ecologically driven aerodynamic function would be highly unlikely to produce optimum aerodynamic functionality. The similarity in aerodynamic optimisations apparent in the various families of bats presented here is consistent with the assumption that the model linking morphological variables to flight speed and wingbeat kinematics is functionally based, rather than an aerodynamically trivial artefact of phylogenetic relationships (Felsenstein, 1982; McKenzie et al., 1995b).

The pooled species data included in this study show $f_w$ values ranging from 3 to 12 Hz. Species with $f_w$ values up to 12 Hz probably have downstroke and upstroke muscles composed of the fast fibre type (Guyton and Hall, 1996). In species with $f_w$ values down to 3 Hz, it is possible that the slow fibre type dominates. This hypothesis is based on our observation that the larger bats with slow wingbeat frequencies are those that are known to travel long distances (*Pteropus poliocephalus*, refer to Churchill, 1998; *Saccolaimus flaviventris*, refer to Strahan, 1995; *Tadarida australis*, refer to Churchill, 1998) or migrate on an annual cycle. Further work is recommended to confirm this suggestion.

The variation of $f_w$ with flight speed for these 23 species shows a two-stage characteristic that is reflected by the need for a logarithmic equation (e.g. Fig. 6). At low speeds, $f_w$ changes with flight speed, whereas at higher speeds it is nearly constant. This is consistent with the rule that only a limited range of wingbeat frequencies are available to a species (Rayner, 1985) to provide the endurance required for long sustained flights. Initially, $f_w$ decreases as flight speed increases, until cruising speed ranges are reached (see mode speed data in Table 3). The reduction is small, approximately 2 Hz. At and above cruising speed, $f_w$ appears to remain almost constant until the bats reach their extreme high speed (e.g. Figs 2 and 6). In contrast to bats,

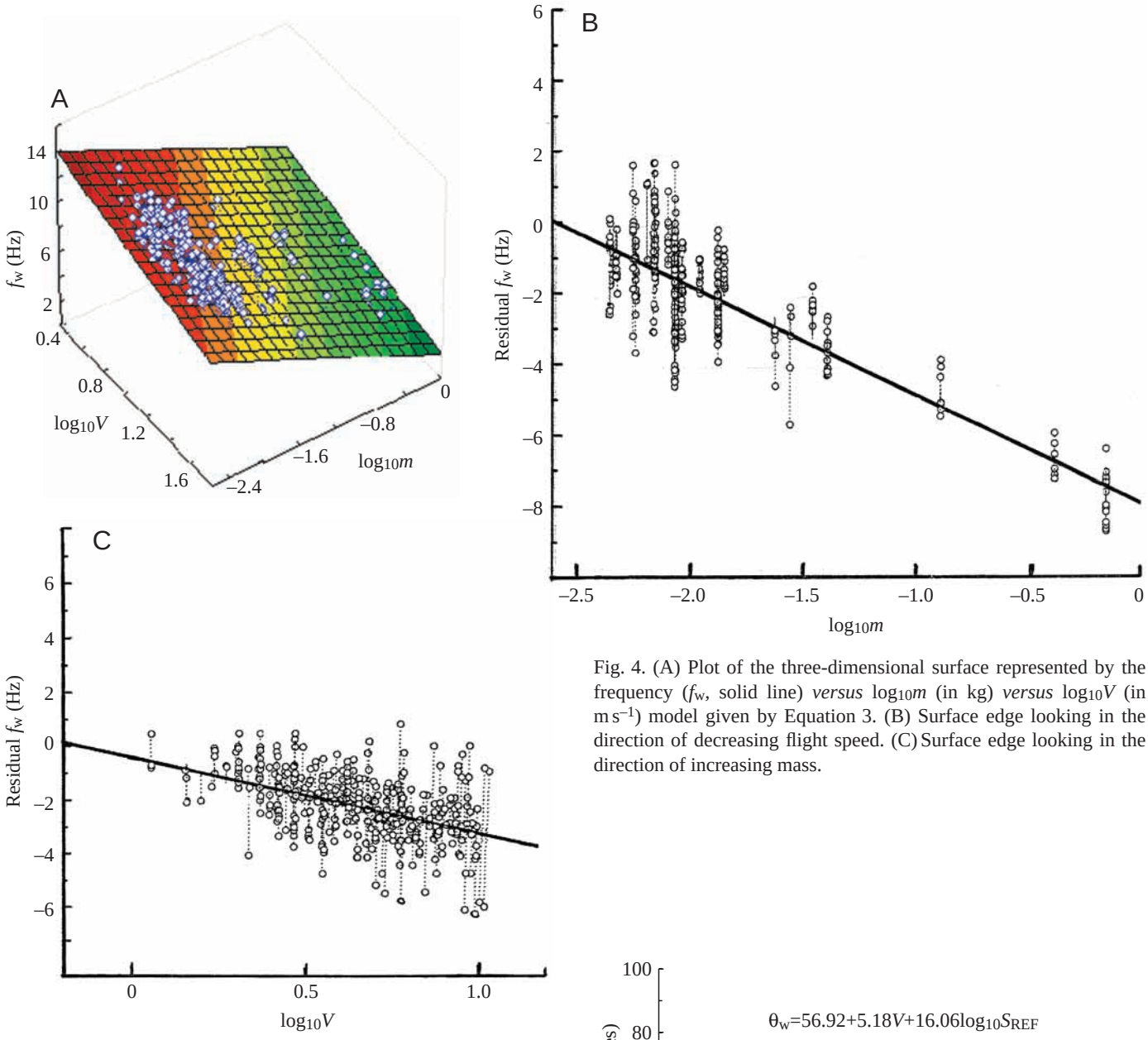


Fig. 4. (A) Plot of the three-dimensional surface represented by the frequency ($f_w$, solid line) *versus* $\log_{10}m$ (in kg) *versus* $\log_{10}V$ (in $m\,s^{-1}$) model given by Equation 3. (B) Surface edge looking in the direction of decreasing flight speed. (C) Surface edge looking in the direction of increasing mass.

bird flight is more variable. Some birds show no change with speed (Tobalske and Dial, 1996), others show a more-or-less linear relationship with speed (Tobalske, 1995) and still others show a U-shaped relationship, with an initial fall in $f_w$ with increasing speed followed by an increase of $f_w$ at even higher speeds (Bruderer et al., 2001; Park et al., 2001). The two-stage relationship in bats differs from published bird data. This almost constant relationship between $f_w$ and flight speed at high speed in the bats we have assessed may be due to use of their most efficient muscle contraction frequency in the flight speed region of rapidly increasing 'opposing loading' and, therefore, metabolic power requirement. The opposing loading applied to the muscles is due to the rapidly increasing drag airloads.

For low-speed $f_w$ data, the model predicts a value that lies in the centre of the scatter of the available empirical data for

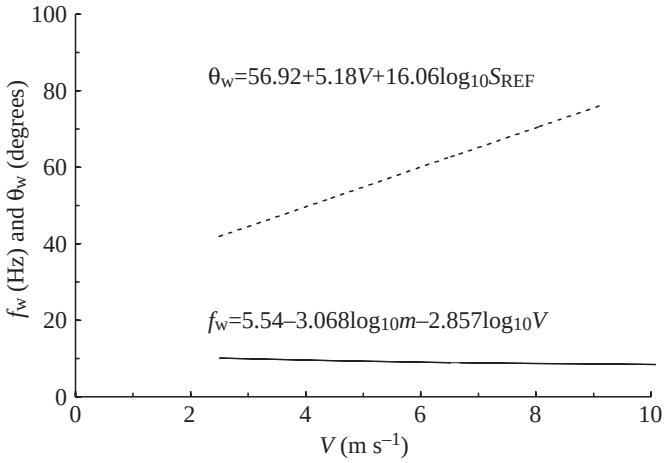


Fig. 5. Proposed model for wingbeat frequency ($f_w$, solid line) and amplitude ($\theta_w$, broken line) variation with mass and flight speed ($V$). For clarity and for direct comparison with the data in Fig. 2, the model for *Chalinolobus gouldii* of mass ($m$) 0.0134 kg is presented. $S_{REF}$ is wing area in $m^2$.

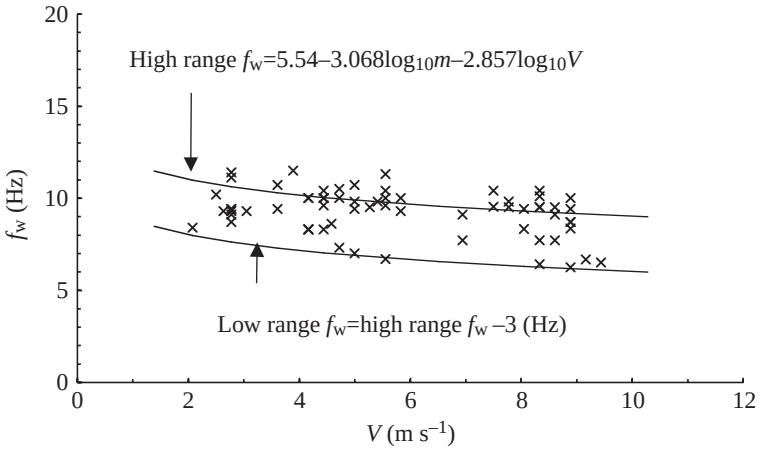


Fig. 6. Wingbeat frequency ($f_w$) data for *Mormopterus planiceps*. Equation 3 describing the general relationship between $f_w$, mass ($m$) and flight speed ($V$) is superimposed over the data, showing the accurate prediction of the higher frequency range used by the bat. For this species, a lower $f_w$ range, approximately 3 Hz below the Equation 3 estimate, is also used by the bat. This is the only species observed to use two different frequency ranges.

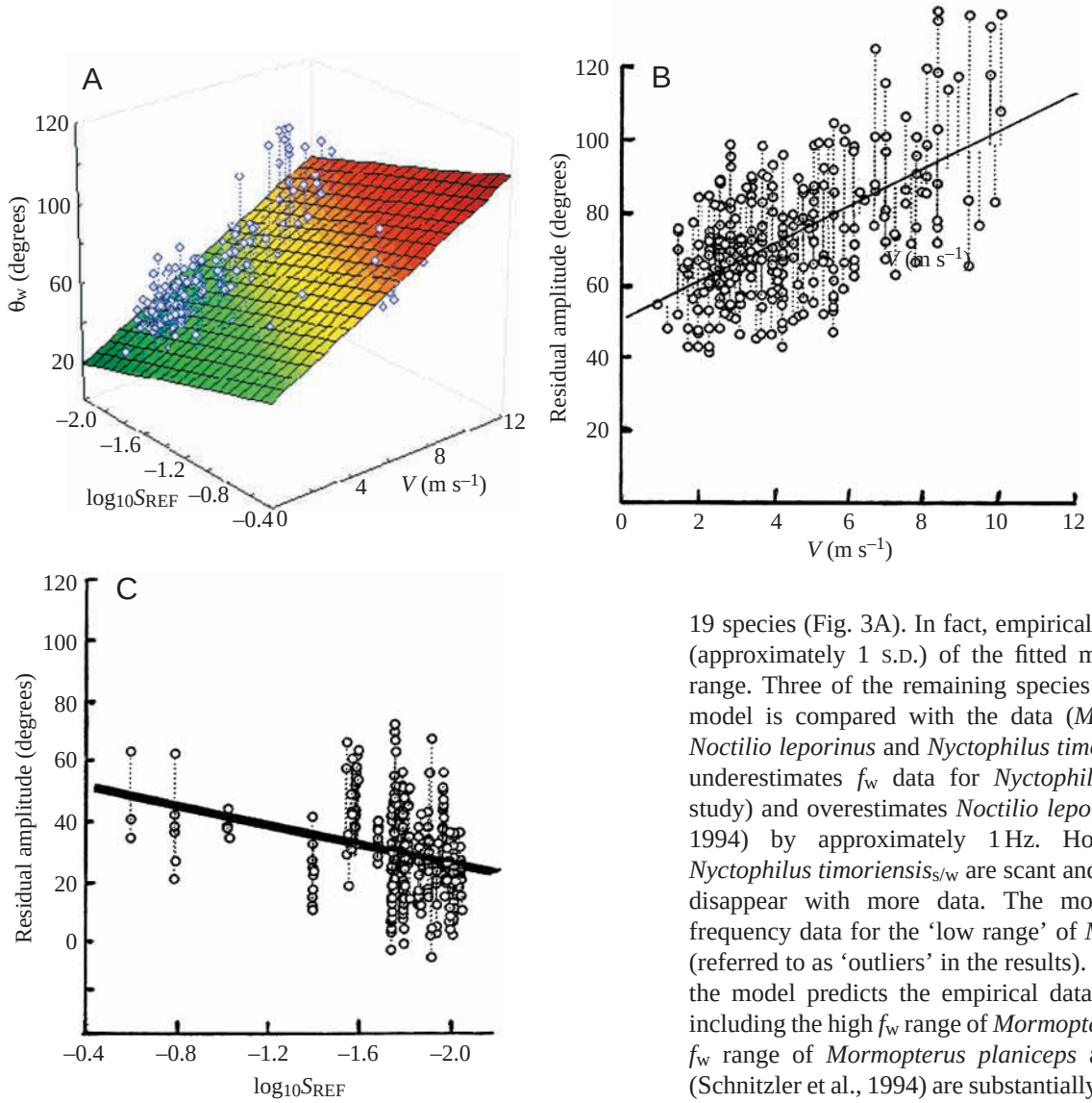


Fig. 7. (A) Plot of the three-dimensional surface represented by the wingbeat amplitude ($\theta_w$) *versus* flight speed ($V$) *versus* log$_{10}S_{REF}$ (in m$^2$) model given by Equation 4. (B) Surface edge looking in the direction of decreasing area. (C) Surface edge looking in the direction of decreasing flight speed.

19 species (Fig. 3A). In fact, empirical values are within 1 Hz (approximately 1 S.D.) of the fitted model across the speed range. Three of the remaining species show a bias when the model is compared with the data (*Mormopterus planiceps*, *Noctilio leporinus* and *Nyctophilus timoriensis*$_{s/w}$). The model underestimates $f_w$ data for *Nyctophilus timoriensis*$_{s/w}$ (this study) and overestimates *Noctilio leporinus* (Schnitzler et al., 1994) by approximately 1 Hz. However, our data on *Nyctophilus timoriensis*$_{s/w}$ are scant and the apparent bias may disappear with more data. The model overestimates the frequency data for the 'low range' of *Mormopterus planiceps* (referred to as 'outliers' in the results). For high-speed $f_w$ data, the model predicts the empirical data for 18 of 19 species, including the high $f_w$ range of *Mormopterus planiceps*. The low $f_w$ range of *Mormopterus planiceps* and *Noctilio leporinus* (Schnitzler et al., 1994) are substantially overestimated. In both species, empirical wingbeat frequencies are approximately 65 % of the value predicted by the model.

*Mormopterus planiceps* was unique among the 23 species assessed during this study. The empirical $f_w$ data are arrayed in two parallel series across the full flight speed range (Fig. 6). The

Table 5. *Maximum and minimum values of wingbeat amplitude for the species included in the study*

| Species | Amplitude (degrees) | | | | | |
|---|---|---|---|---|---|---|
| | Minimum recorded | Minimum, first percentile | Maximum recorded | Maximum 99th percentile | Maximum range | First to 99th percentile range |
| *Chalinolobus gouldii* | –90 | –90 | 60 | 50 | 150 | 140.0 |
| *Chalinolobus morio* | –90 | –80 | 50 | 45 | 140 | 125.0 |
| *Chalinolobus nigrogriseus* | –80 | –80 | 65 | 63.2 | 145 | 143.2 |
| *Hipposideros ater* | –60 | –51.3 | 55 | 50 | 115 | 101.3 |
| *Macroderma gigas* | –65 | –65 | 60 | 60 | 125 | 125 |
| *Miniopterus schreibersii* | –70 | –70 | 60 | 60 | 130 | 130 |
| *Mormopterus planiceps* | –65 | –50 | 60 | 50 | 125 | 100 |
| *Nyctophilus arnhemensis* | –60 | –40 | 50 | 41.5 | 110 | 81.5 |
| *Nyctophilus geoffroyi* | –85 | –83.1 | 65 | 56.8 | 150 | 139.9 |
| *Nyctophilus gouldi* | –70 | –60 | 50 | 50 | 125 | 110 |
| *Nyctophilus timoriensis*$_{g}$ | –80 | –72.7 | 50 | 46.5 | 130 | 119.2 |
| *Nyctophilus timoriensis*$_{s/w}$ | –45 | –40 | 50 | 50 | 95 | 90 |
| *Pteropus poliocephalus* | –80 | –80 | 55 | 54 | 135 | 134 |
| *Pteropus scapulatus* | –80 | –80 | 70 | 68.1 | 150 | 148.1 |
| *Rhinonycteris aurantius* | –60 | –60 | 50 | 50 | 110 | 110 |
| *Saccolaimus flaviventris* | –60 | –60 | 50 | 50 | 110 | 110 |
| *Scotorepens balstoni* | –60 | –50.7 | 50 | 50 | 110 | 100.7 |
| *Scotorepens greyi* | –80 | –73.7 | 55 | 51.7 | 135 | 125.4 |
| *Tadarida australis* | –90 | –82.7 | 60 | 60 | 150 | 142.7 |
| *Taphozous georgianus* | –60 | –57.9 | 60 | 60 | 120 | 117.9 |
| *Taphozous hilli* | –85 | –82 | 55 | 55 | 140 | 137.0 |
| *Vespadelus finlaysoni* | –80 | –80 | 50 | 45.7 | 130 | 125.7 |
| *Vespadelus regulus* | –60 | –55 | 50 | 47.3 | 110 | 102.3 |

Data are pooled from all Western Australian regions.
Data presented are the absolute maximum and minimum values observed together with the first and 99th percentile values.
Note that the number of wingbeat cycles is given in Table 4.
Refer to Materials and methods for the explanation of the two different populations of *Nyctophilus timoriensis*.

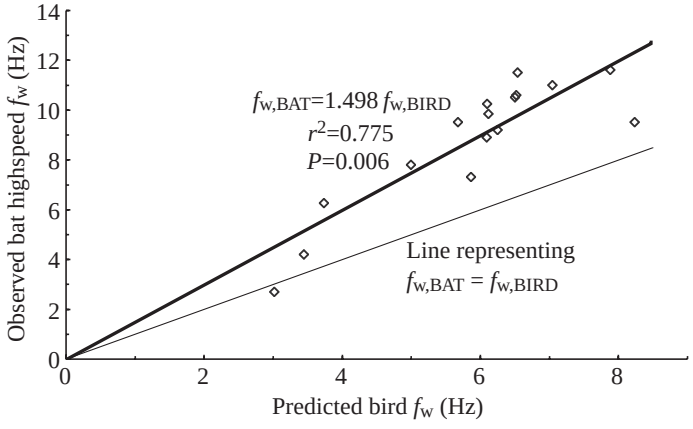


Fig. 8. Comparison of bat wingbeat frequency ($f_w$) data with bird kinematics. For each bat species included in this study, the observed high-speed $f_w$ is plotted against a $f_w$ value calculated using the model applicable to birds from Pennycuick (1996). The values of the bat's mass, span and wing area from Table 1 are used for the calculated frequency. The upper bold line represents a regression showing that bat $f_w$ is 50 % higher than bird $f_w$ of similar morphological values. The lower thin line gives a hypothetical line of equivalence.

model predicted the main (higher) frequency series. The other series averaged 3 Hz lower and, provided that it is not a sampling artifact, would reduce the resultant airspeed past the wing during the down- and upstroke. Preliminary calculations indicate a consequent reduction in the profile power fraction of the wing of approximately 4 % and in the inertial power fraction of 67 %. Preliminary dissections by the authors also revealed that *Mormopterus planiceps* has a very low flight muscle mass to total mass fraction of wing down-stroke and up-stroke muscle groups (Vaughan, 1970; Hermanson and Altenbach, 1985), approximately 7.5 % of total mass compared with a more typical range of approximately 9–11 % for similar insectivores. Taken together, these observations suggest a particular optimisation of this tiny interceptor, in which the upper $f_w$ series is used for acceleration to speed and for manoeuvring to intercept prey, while the lower $f_w$ range is used for efficient cruising/commuting.

By comparison with birds, bats have a 50 % higher wingbeat frequency for a given size range. Pennycuick (1996) gives a model for bird frequency based upon mass, wing span and wing area. This model is compared with our high-speed bat data in Fig. 8.

We had empirical data on $\theta_w$ for 24 species (including *Rhinolophus ferrumequinum* (Aldridge, 1986)). No species

departed substantially from the general model given by Equation 4. However, unlike $f_w$, all species showed a high level of scatter (±20 °) in the raw amplitude data (e.g. Fig. 2), forming effectively two blocks that represent the low- and high-speed experimental data collection strategies (see Fig. 2). The bats were studied in free flight at all times, during which climbing, descending, accelerating and decelerating flight would require differences in lift, drag and thrust. It is possible for the bat to generate lift and thrust by changing the mean wingbeat angle of attack ($\alpha$), the average airspeed over the wings ($V_{wing}$), the wingbeat frequency and/or amplitude. At low angles of attack, lift is directly proportional to the product of $\alpha$ and $V_{wing}^2$. For level flight, when lift exactly equals weight, the bat must change the flow velocity over its wings by changing forward speed, $f_w$ and/or $\theta_w$ if it changes its mean wing $\alpha$ during the stroke, otherwise, it will climb or descend. In addition, to increase speed in level flight, the bat must generate more thrust by using higher $\alpha$, $f_w$ and/or $\theta_w$ to offset the increasing drag. Given that we have shown that $f_w$ is relatively constant across the full speed range of bats, $\alpha$ must decrease as flight speed increases (for constant or increasing $\theta_w$) otherwise the bat will generate excess lift and climb. To this end, wingbeat amplitude must increase to generate the increased thrust, resulting in an even higher mean $V_{wing}$ value and an even lower mean value of $\alpha$. Equation 4 therefore represents the steady level-flight wingbeat amplitude independent of the experimental context in which the data were collected. Note that the previous study (Aldridge, 1986) published data on $\theta_w$ of bats over a narrow range of speeds (2.7–4.8 m s$^{-1}$) using a flight tunnel. These data fall within the predictions of our equation.

The difference between data recorded at 24 frames s$^{-1}$ compared with higher frame rates is given in Table 6 and can be seen in Fig. 1. At high wingbeat frequencies (>9.5 Hz), VHS video camera or a cine camera with 24 frames s$^{-1}$ and a slow shutter speed give an accurate representation of the extrema of the wing positional angle, because they occur at a repetition rate that ensures a high probability of the extrema coinciding with the relatively long open shutter/scan time period. These extrema are then used as the frame $\theta_w$ value. Similarly, 24 frames s$^{-1}$ is sufficient to capture relatively slowly moving wings at low $f_w$ (<7 Hz) within 5 ° of its maximum position (see Fig. 1C). There is, however, a range of wing frequencies (approximately 7–9.5 Hz) used by bats of 20–50 g to which neither of these situations applies. For these bats, care must be taken to use only the 24 frames s$^{-1}$ frame images that clearly show a significant variation in angle from frame to frame. Frames that do not fit this criterion should not be included in averaging $\theta_w$ values for the test point. This effect is apparent in the *Tadarida australis* data of Table 6, which underestimate actual amplitude by 10–20 °. Underestimation occurred in four of our bats: *Taphozous hilli*, *Taphozous georgianus*, *Tadarida australis* and *Saccolaimus. flaviventris*. Even so, this bias is of the same order as the overall scatter in the data collected, and the data for these species have therefore been included in the overall regression analysis. Fig. 7C shows that including these data has little effect on the regression result. Data from Fig. 1A

Table 6. *Comparison of wingbeat amplitudes derived at different frame rates for three species flying at low speeds in the observation chamber*

| | | | Wingbeat amplitude (degrees) | | | | | | | | |
|---|---|---|---|---|---|---|---|---|---|---|---|
| | | | Cine at 200 frames s$^{-1}$ | | | DigiBeta into VHS at 48 frames s$^{-1}$ | | | VHS at 24 frames s$^{-1}$ | | |
| Species | Flight speed $V$ (m s$^{-1}$) | Wingbeat frequency $f_w$ (Hz) | Range | Maximum | Minimum | Range | Maximum | Minimum | Range | Maximum | Minimum |
| *Vespadelus regulus* | 3.3 | 10.4 | 29.2 to –29 | 35 | –45 | 22 to –30 | 30 | –40 | 22.5 to –30 | 30 | –40 |
| *Chalinolobus gouldii* | 2.9 | 10.7 | 38.3 to –22.5 | 40 | –25 | 41.7 to –20 | 45 | –20 | 41.7 to –16.7 | 45 | –20 |
| *Chalinolobus gouldii* | 2.6 | 12.0 | 33.8 to –10 | 40 | –15 | 30 to –13.3 | 40 | –20 | 30 to –13.3 | 40 | –20 |
| *Tadarida australis* | 5.4 | 8.9 | 44.2 to –80 | 50 | –90 | 35 to –61.7 | 45 | –80 | 33 to –55 | 40 | –70 |
| *Tadarida australis* | 5.2 | 9.0 | 46 to –36.7 | 50 | –80 | 37 to –41.7 | 45 | –60 | 39 to –41.7 | 45 | –60 |

There is good correlation between amplitude values derived at high wingbeat frequencies (>9.5 Hz). The mid-range represented by *Tadarida australis* shows that frame rates significantly faster than 48 frames s$^{-1}$ are required to capture the full range and maxima used by the bat.

show that this effect is reduced at frame rates of 50 frames $s^{-1}$ and is not apparent at rates beyond 100 frames $s^{-1}$.

Field observations of bats 'hand-released' in daylight (Table 5) suggest that bats approach their amplitude limits of approximately 50–60 ° above and 80–90 ° below the reference dorsal plane in extreme flight conditions. This gives a theoretical maximum of 140–150 ° for wingbeat amplitude at the high speed extreme of the flight speed range, compared with a more typical range of 40–80 °. This theoretical maximum will be influenced by the back, shoulder, elbow and wrist morphology of the various species. Given that maximum efficiency in skeletal muscle ordinarily occurs when the velocity of contraction is approximately 30 % of maximum (Guyton and Hall, 1996) and that $f_w$ is virtually constant in the bat's upper speed range, our result of a threefold increase in amplitude at extreme speeds is consistent with constant $f_w$ and best use of muscle efficiency in the bat's normal speed range.

The relationships between $f_w$, $\theta_w$ and flight speed are defined by two simple equations involving mass and wing area. The same equations fitted tropical as well as temperate species, megabats and microbats, the six microbat families assessed and species with the full range of foraging ecologies. One scaling model fitted all. Its simplicity implies that a single theme underlies bat aerodynamics. This argument is not circular because no bats showed substantial departures from the model, despite differences in foraging niche, climatic range and phylogeny. In this respect at least, the kinematics of bat flight is different from that of birds.

## List of symbols

| | |
|---|---|
| $f_w$ | Wingbeat frequency (Hz) |
| $m$ | Bat mass (kg) |
| $S_{REF}$ | *W*ing reference area ($m^2$) |
| $V_{mr}$ | Maximum range flight speed ($m\,s^{-1}$) |
| $V_{mode}$ | Flight speed representing the 'mode' speed of the test data ($m\,s^{-1}$) |
| $V_{wing}$ | Resultant airspeed over the wing including contributions from flight speed, wingbeat frequency and amplitude ($m\,s^{-1}$) |
| $\alpha$ | Angle of attack (degrees) |
| $\theta_w$ | Wingbeat amplitude (degrees) |

We thank C. L. Bullen, M. H. McKenzie, W. P. Muir and A. N. Start for field assistance. Daniel Searle, Sarah Neylon and Ingo Helbig of Storyteller Productions, Perth, Western Australia, assisted with the photography. Mike Searle kindly made his visual technology production facilities available to us for data reduction and analysis. The Western Australian Department of Conservation and Land Management contributed to the cost of the project. We also thank two anonymous referees for constructive comments on an earlier manuscript.

## References

**Aldridge, H. D. J. N.** (1986). Kinematics and aerodynamics of the greater horseshoe bat, *Rhinolophus ferrumequinum*, in horizontal flight at various flight speeds. *J. Exp. Biol.* **126**, 479–497.

**Britton, A. R. C., Jones, G., Rayner, J. M. V., Boonman, A. M. and Verboom, B.** (1997). Flight performance, echolocation and foraging behavior in pond bats, *Myotis dasycneme*. *J. Zool., Lond.* **241**, 503–522.

**Bruderer, L., Liechti, F. and Bilo, D.** (2001). Flexibility in flight behavior of barn swallows (*Hirundo rustica*) and house martins (*Delichon urbica*) tested in a wind tunnel. *J. Exp. Biol.* **204**, 1473–1484.

**Bullen, R. D. and McKenzie, N. L.** (2001). Bat airframe design – flight performance, stability and control in relation to foraging ecology. *Aust. J. Zool.* **49**, 235–261.

**Carpenter, R. E.** (1985). Flight physiology of flying foxes, *Pteropus poliocephalus*. *J. Exp. Biol.* **114**, 619–647.

**Carpenter, R. E.** (1986). Flight physiology of intermediate-sized fruit bats (Pteropodidae). *J. Exp. Biol.* **120**, 79–103.

**Churchill, S.** (1998). *Australian Bats.* Sydney: Reed New Holland.

**Felsenstein, J.** (1982). Numerical methods for inferring evolutionary trees. *Quart. Rev. Biol.* **57**, 379–404.

**Fenton, M. B.** (1982). Echolocation calls and patterns of hunting and habitat use of bats (Microchiroptera) from Chillagoe, North Queensland. *Aust. J. Zool.* **30**, 417–425.

**Fullard, J., Koehler, K., Surlykke, A. and McKenzie, N. L.** (1991). Echolocation ecology and flight morphology of insectivorous bats (Chiroptera) in southwestern Australia. *Aust. J. Zool.* **39**, 427–438.

**Guyton, A. C. and Hall, J. E.** (1996). *Textbook of Medical Physiology*. Ninth edition. Philadelphia: W. B. Saunders Company.

**Hermanson, J. W. and Altenbach, J. S.** (1985). Functional anatomy of the shoulder and arm of the fruit eating bat *Artibeus jamaicensis*. *J. Zool., Lond. A* **205**, 157–177.

**Lancaster, W., Henson, O. and Keating, A.** (1995). Respiratory muscle activity in relation to vocalisation in flying bats. *J. Exp. Biol.* **198**, 175–191.

**McKenzie, N. L. and Start, A. N.** (1989). Structure of bat guilds in mangroves: environmental disturbances and determinism. In *Patterns in the Structure of Mammalian Communities* (ed. D. W. Morris, Z. Abramski, B. J. Fox and R. Willig), pp. 167–178. Lubbock: Texas Technical University.

**McKenzie, N. L., Fontanini, L., Lindus, N. V. and Williams, M. R.** (1995a). Biological inventory of Koolan Island, Western Australia 2. Zoological notes. *Rec. West. Aust. Mus.* **17**, 249–266.

**McKenzie, N. L., Gunnell, A., Yani, M. and Williams, M.** (1995b). Correspondence between flight morphology and foraging ecology in some Palaeotropical bats. *Aust. J. Zool.* **43**, 241–257.

**McKenzie, N. L. and Muir, W. P.** (2000). Bats of the southern Carnarvon basin, Western Australia. *Rec. West. Aust. Mus. (Suppl.)* **61**, 465–477.

**Norberg, U. M.** (1976). Aerodynamics, kinematics and energetics of horizontal flapping flight in the long eared bat *Plecotus auritus*. *J. Exp. Biol.* **65**, 179–212.

**Norberg, U. M., Kunz, T. H., Steffensen, J. F., Winter, Y. and von Helversen, O.** (1993). The cost of hovering and forward flight in a nectar-feeding bat, *Glossophagia soricina*, estimated from aerodynamic theory. *J. Exp. Biol.* **182**, 207–227.

**Park, K. J., Rosen, M. and Hedenstrom, A.** (2001). Flight kinematics of the barn swallow *(Hirundo rustica)* over a wide range of speeds in a wind tunnel. *J. Exp. Biol.* **204**, 2741–2750.

**Pennycuick, C. J.** (1989). *Bird Flight Performance. A Practical Calculation Manual*. Oxford: Oxford University Press.

**Pennycuick, C. J.** (1996). Wingbeat frequency of birds in steady cruising flight: new and improved predictions. *J. Exp. Biol.* **199**, 1613–1618.

**Rayner, J. M. V.** (1985). Bounding and undulating flight in birds. *J. Theor. Biol.* **117**, 47–77.

**Schnitzler, H. U., Kalko, E. K. V., Kaipf, I. and Grinnell, A. D.** (1994). Fishing and echolocation behavior of the greater bulldog bat, *Noctilio leporinus*, in the field. *Behav. Ecol. Sociobiol.* **35**, 327–345.

**Strahan, R.** (ed.) (1995). *The Mammals of Australia*. Sydney: Reed Books.

**Thomas, A. L. R., Jones, G., Rayner, J. M. V. and Hughes, P. M.** (1990). Intermittent gliding flight in the pipistrelle bat (*Pipistrellus pipistrellus*). *J. Exp. Biol.* **149**, 407–416.

**Tobalske, B. W.** (1995). Neuromuscular control and kinematics of intermittent flight in the european starling (*Sturnus vulgaris*). *J. Exp. Biol.* **198**, 1259–1273.

**Tobalske, B. W. and Dial, K. P.** (1996). Flight kinematics of black-billed magpies and pigeons over a wide range of speeds. *J. Exp. Biol.* **199**, 263–280.

**Van Den Berg, C. and Rayner, J. M. V.** (1995). The moment of inertia of bird wings and the inertial power requirement for flapping flight. *J. Exp. Biol.* **198**, 1655–1664.

**Vaughan, T. A.** (1970). The muscular system. In *Biology of Bats*, vol. 1 (ed. W. A. Wimsatt), pp. 140–193. New York: Academic Press.